Title	Probing the low-temperature chemistry of ethanol via the addition of dimethyl ether
Author(s)	Zhang, Yingjia; El-Merhubi, Hilal; Lefort, Benoîte; Le Moyne, Luis; Curran, Henry J.; Kéromnès, Alan
Publication Date	2017-11-28
Publication Information	Zhang, Yingjia, El-Merhubi, Hilal, Lefort, Benoîte, Le Moyne, Luis, Curran, Henry J., & Kéromnès, Alan. (2018). Probing the low-temperature chemistry of ethanol via the addition of dimethyl ether. Combustion and Flame, 190, 74-86. doi: 10.1016/j.combustflame.2017.11.011
Publisher	Elsevier
Link to publisher's version	https://doi.org/10.1016/j.combustflame.2017.11.011
Item record	http://hdl.handle.net/10379/14790
DOI	http://dx.doi.org/10.1016/j.combustflame.2017.11.011

An Experimental and Kinetic Modeling Study of Ethanol/DME Mixtures Auto-Ignition

Y. Zhang[1,2], H. El-Merhubi[3], B. Lefort[3], L. Le Moyne[3], H.J. Curran[1], A. Kéromnès[3]*
[1]Combustion Chemistry Centre, National University of Ireland Galway, Ireland
[2]State Key Laboratory of Multiphase Flow in Power Engineering, Xi'an Jiaotong University, Xi'an 710049, China
[3]DRIVE EA1859, Univ. Bourgogne Franche Comté, F58000 Nevers, France

Abstract

Ignition delay times of ethanol/DME/air mixtures were measured in a rapid compression machine and in two high-pressure shock tubes at conditions relevant to internal combustion engines. The influences of these conditions on the auto-ignition behavior of the mixture blends were systematically investigated. Our results indicate that, in the low temperature range (650 – 950 K), increasing the amount of DME in the fuel mixture increases. At higher temperatures, reactivity is controlled by ethanol and there is almost no visible impact of the fuel mixture composition, whereas DME shows a slower reactivity. The experimental measurements were simulated using an updated mechanism for ethanol which includes the latest experimental or theoretical work in the literature. Results indicates that the model is in satisfactory agreement with all of the mixtures.

1. Introduction

Ethanol is considered to be a promising transportation biofuel due to its sustainability [1,2] and low soot emissions [3,4] in internal combustion engine (ICE). In order to consider its potential use in real internal combustion engines, it is important to investigate *a priori* how it will behave under practical engine relevant conditions. Ethanol also has an impact on the reactivity of surrogate fuels [5]. Compared to mixtures made of primary reference fuels (PRF), n-heptane and iso-octane, ethanol reduces the NTC (Negative Temperature Coefficient) behavior at low temperature and increases the reactivity at intermediate and high temperature. Thus, ethanol has been previously extensively studied under various range of conditions including flame speed measurements [6 – 12], ignition delay times measurements in shock tube [13 – 17] and rapid compression machines [17 – 19], species measurements in rapid compression facility [19], flow reactors [5,20,21] and jet-stirred reactors [22]. There is, however, limited experimental data with which to evaluate the auto-ignition behavior of ethanol under engine relevant conditions: high pressure and low to intermediate temperature (especially below 850 K) [18] since most of the experimental investigation has been performed at low pressure (below 5 bar) or at high temperature (above 1000 K). Considering measurements performed at high pressure, Heufer and Olivier [15] measured the ignition delay times of the

*Corresponding author: alan.keromnes@u-bourgogne.fr

stoichiometric ethanol-air mixture at 13, 19, 40 and 75 bar over a temperature range of 910 – 1190 K using a shock tube. Cancino et al. [16] investigated the ignition of for lean ethanol-air mixture (φ = 0.3) at 30 bar between 860 K and 1180 K and for stoichiometric mixture over a pressure range of 10 to 50 bar with a temperature range of 800 K to 1250 K in a shock tube. Lee et al. [17] performed a shock tube and RCM study of stoichiometric ethanol-air mixture under high pressure conditions (67 – 93 bar) in the intermediate temperature range (775 – 1000 K). Mittal et *al.* [18] investigated the auto-ignition behavior of lean ethanol-air mixture (φ = 0.3 and 0.5) in the intermediate temperature range (830 – 980 K) for a pressure range of 10-50 bar and of stoichiometric mixture at 10 bar and over limited temperature range (870 – 920 K). More recently, Barraza-Botet et *al.* [19] measured ignition delay times and species concentration for diluted stoichiometric ethanol/O_2 mixture in a rapid compression facility between 880 K and 1120 K over a pressure range of 3 – 10 bar. Extended experimental work on ethanol ignition, including lean to rich mixtures, has been mainly performed at high temperature and low pressure or diluted conditions in shock tubes [13,23,24]. The available data are summarized in Figure 1. It appears that there is a lack of data at low temperature and high pressure (Figure 1~~Figure 1~~b). This lack of data limits the construction, validation and interpretation of chemical kinetic mechanism for the real combustor design. Such data are particularly important in assessing the influence of blending ethanol with practical fuels, in which the low reactivity of ethanol will inhibit the reactivity of a fuel at these low temperature conditions [25,26]. Moreover, Mittal et al. [18] reveal some discrepancies in the data available at low temperature (Figure 1~~Figure 1~~a) wheras there is a very good agreement at high temperature. They attribute part of this scatter to pre-ignition pressure rise in shock tubes. The recent study from Barraza-Botet et al. [19] suggests that the accuracy of rate constants for ethanol + $H\dot{O}_2$ needs to be improve. This is confirmed by Olm et al. [27] who performed an optimization of ethanol mechanism previously published by Saxena and Williams [9]. Therefore, low temperature chemistry of ethanol might be questionable.

Detailed chemical kinetics mechanisms have been proposed by several authors [7,9,16,17,22,28–31]. Dunphy et al. [28] validated a kinetic mechanism against ignition delay times measurements performed at low pressures (2-4.5 bar) and at high temperatures (1100 – 1500 K). Egolfopoulos et al. [7] proposed a mechanism tested under low pressure conditions including ignition delay times, species profiles measured in flow reactor and laminar flame speeds. Marinov [29] validated his mechanism against a wide range of experimental conditions including laminar flame speeds, species profiles measured in jet-stirred reactor and flow reactor and ignition delay times. Li et al. [30] studied the decomposition of ethanol in a flow reactor and proposed a rate constant for the decomposition reaction $C_2H_5OH = C_2H_4 + H_2O$ in order to improve the mechanism previously developed by Marinov. Saxena and Williams [9] proposed a new mechanism validated at low pressure against flame speeds, ignition delay times and species

profiles. Cancino et al. [16] built their mechanism based on that of Marinov and validated it against ignition delay times under high pressure conditions (10 – 50 bar) for lean and stoichiometric mixtures. Leplat et al. [22] based their mechanism by combining the mechanism developed by Marinov [29] and GRI Mech [32] with previously released new rate constant. They increased the pressure range by testing the mechanisms against jet-stirred reactor and flame speed measured at 10 bar reproduced ignition delay times and species profiles with a good agreement. Lee et al. [17] revisited the mechanism proposed by Li et al. [30] and extended the validation to high pressure (80 bar) based on ignition delay times measurements performed in high-pressure shock tube and rapid compression machine for stoichiometric ethanol-air mixtures. Metcalfe et al. [31] proposed a C1–C2 mechanism validated against a wide range of conditions including ethanol combustion targets.

In the present study, ignition delay times have been measured in rapid compression machine and in shock tubes covering lean to rich conditions (φ = 0.5, 1.0 and 2.0) over a wide range of temperature (650 – 1250 K) under pressure conditions relevant to internal combustion engines (20 and 40 bar). However, due to limitations of experimental facilities (especially heat transfer), it is difficult to measure long ignition delay times at temperature below 825 K for ethanol-air mixture. Recently, in order to probe its low temperature chemistry, toluene was blended with dimethyl ether (DME) in order to test a mechanisms ability to reproduce accurately the reactivity of various binary mixture combinations [33]. Due to the success of that study, DME has been selected as a radical initiator once again to test the predictive capability of a mechanism to accurately reproduce the experimentally observed reactivity of binary ethanol/DME mixtures and extend the temperature range to 650 K. In order to assess the inhibiting effect of ethanol, different blending ratios have been tested: ethanol/DME: 0/100, 50/50, 30/70, 100/0. Using this experimental database, the chemical kinetic mechanism has been revised and its performance has been evaluated against these binary mixtures and data available in the literature.

In the following sections, the experimental devices are described, followed by a presentation and a discussion of the experimental results. Then, the revised chemical kinetic mechanism is presented and its performances in reproducing experimental results is discussed.

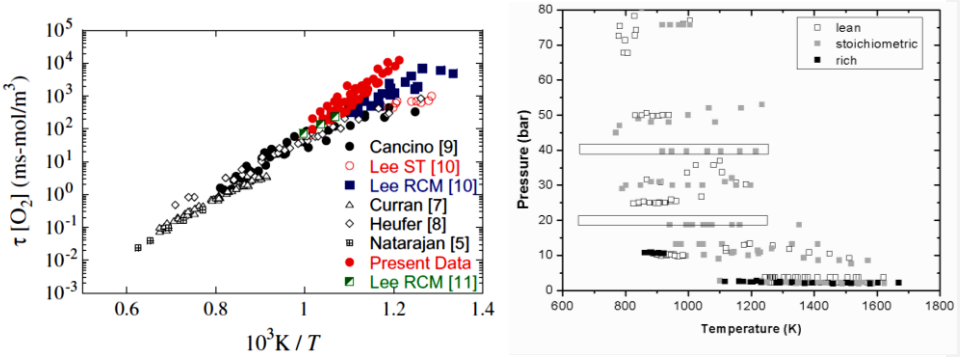

Figure 1: Comparison of the available ignition delay times data (symbols) with the experimental conditions presented in this study

2. Experimental devices

The experiments were carried out in a rapid compression machine (RCM) in NUI Galway and two high-pressure shock tubes (NUI Galway and DRIVE). Ignition delay times of ethanol/DME/air mixtures were measured at conditions relevant to those encountered in ICEs (pressure: 20 – 40 bar, temperature: 650 – 1250 K, equivalence ratio: 0.5 – 2.0, and blending ratio: ethanol/DME: 0/100, 50/50, 30/70, 100/0 in air). All mixtures were prepared manometrically in heated stainless steel tanks. The partial pressure of ethanol is maintained below one third of its vapor pressure in order to avoid any condensation of the fuels in the tanks. Moreover, all of the intake manifolds, the RCM and the two HPSTs are heated for the same purpose. Ethanol used in *this study* was from Sigma-Aldrich at 99.5 +% purity and O_2, N_2 and He were supplied by BOC Ireland and Air Liquide at 99.5%, 99.95% and 99.9%, respectively.

The RCM is a horizontally-opposed twin-piston device that has been described previously [34,35]. The symmetry of the RCM allows a short adiabatic compression process (16 – 17 ms) and helps to reduce the aerodynamic effects inside the combustion chamber at the end of the compression process [36]. Moreover, the piston heads include a crevice shape which captures the vortex created by the piston corner compression. Thus, the mixture and the temperature are homogeneous prior to ignition. The pressures and temperatures achieved at the end of the compression process (p_C and T_C respectively) in this study were 20 and 40 bar and 650 – 1050 K, respectively. The final conditions were reached by changing the initial pressure and temperature. For all experiments, the pressure and the position of both pistons are recorded using a digital oscilloscope. The pressure profile recorded with a pressure transducer (Kistler 603B) provided the compression time and was used to measure the ignition delay time.

It was defined as the time difference between the end of the compression process and the maximum rate of increase of the pressure. The temperature, T_C, is calculated using the initial temperature, T_i, and pressure, p_i, and the pressure, p_C, assuming adiabatic compression and frozen chemistry and using Gaseq [37]. For each experimental conditions, an experiment with a non-reactive mixture was performed by replacing oxygen by nitrogen in the test mixture since they have similar thermodynamic properties. The recorded pressure profile is used in order to take into account heat losses when simulating the experiments.

The experiments in DRIVE were carried out in a high-pressure shock tube which has been previously described [38]. The stainless steel tube has an inner diameter of 50 mm and is divided by a double membrane (stainless steel diaphragm) into two sections (a driver section of 4 m and a driven section of 5 m) constituting a small section called "intermediate section (IS)". In addition of the main tube, this facility includes a vacuum system (a roughing pump and a turbo-molecular pump) which pumped down the tube and the stainless steel tanks to pressures below 5 Pa, a velocity detection system (based on four individual piezoelectric pressure transducers PCB 113B22) and a data acquisition system (NI Compact RIO). The tube, mixing tanks and manifold were pre-heated to 80°C to avoid any condensation of ethanol by ensuring its partial pressure is below one third of its vapor pressure. Post-shock pressures, p_5, are measured using a Kistler piezoelectric pressure transducer (603B1) located at the endwall. The temperature, T_5, behind the reflected shock wave is calculated using the shock wave velocity in conjunction with the 1-D shock relations and the species thermodynamics using the chemical equilibrium software Gaseq [37] with an accuracy of ±1% which corresponds to ±10 – 15 K. The Kistler pressure transducer is also used to determine the qualitative, transient pressure and to determine the ignition delay time. It is defined as the time interval between the time when the pressure and temperature conditions behind the reflected shock wave are reached and the onset of combustion, commonly defined by sudden change in pressure.

Only ignition delay times of ethanol/air mixture at 20 and 40 atm at φ = 1.0 were measured in the NUI Galway HPST, described previously [39], in order to cross-check the reliability of the data recorded in both facilities. Briefly, the HPST has a constant inner diameter of 63.5 mm with a 3.0 m driver section and a 5.7 m driven section. Two pre-scored aluminum diaphragms were used to promote an ideal bursting and minimize undesirable fluid dynamics during incident shock formation. The tube, mixing tank and manifold were pre-heated to 75 °C to allow the partial pressure of ethanol in the prepared mixture was four times less than its vapor pressure. The prepared mixtures were allowed to diffusively mix for 12 hours before performing experiments. The end-wall pressures, monitored by a Kistler 603B pressure transducer, were used to identify the ignition delay times. The reflected shock conditions were calculated using Gaseq [37] with input of the measured incident shock velocity determined by six

PCB 113B24 pressure transduces. The largest uncertainties presented here were estimated to be ±15% for ignition delay times and ±20 K in reflected shock temperatures.

All mixtures were tested in the RCM in order to measure the ignition delay times in the low temperature range. For the experiments at higher temperatures, they were performed in the DRIVE high-pressure shock tube except the mixture without ethanol which were previously measured in NUIG [40]. However, in order to complete the database, ignition delay times of DME were measured in DRIVE at 40 bar and φ = 1 and 2. Moreover, the experiments without DME were measured in both shock tubes to allow the comparison of experimental results and showed good agreement. The test matrix is detailed in Table 1~~Table 1~~.

Table 1: Mixtures investigated in this study

Equivalence ratio (φ)	DME (%)	Ethanol (%)	O_2 (%)	N_2 (%)	Device
0.5	–	3.38	20.29	76.33	NUIG RCM & ST + DRIVE ST
	1.01	2.37	20.29	76.33	NUIG RCM + DRIVE ST
	1.69	1.69	20.29	76.33	NUIG RCM + DRIVE ST
	3.38	–	20.29	76.33	NUIG RCM & ST
1.0	–	6.54	19.63	73.83	NUIG RCM + DRIVE ST
	1.96	4.58	19.63	73.83	NUIG RCM + DRIVE ST
	3.27	3.27	19.63	73.83	NUIG RCM + DRIVE ST
	6.54	–	19.63	73.83	NUIG RCM + DRIVE ST
2.0	–	12.28	18.42	69.30	NUIG RCM + DRIVE ST
	3.68	8.60	18.42	69.30	NUIG RCM + DRIVE ST
	6.14	6.14	18.42	69.30	NUIG RCM + DRIVE ST
	12.28	–	18.42	69.30	NUIG RCM + DRIVE ST

3. Update of chemical kinetic mechanism

The base mechanism used in the current study is taken from AramcoMech 1.3, which includes the $H_2/CO/O_2$ sub-mechanism developed by Kéromnès et al. [41] and the C1 – C2 sub-mechanism established by Metcalfe et al.[42]. The sub-mechanisms of ethanol and DME are adopted from the recent work of Mittal et al. [18] and Burke et al. [40] respectively. The original model shows an acceptable prediction at high temperatures whereas it appears to be unsatisfactory in simulating these new ignition delay time data measured in this study. Particularly for 50% EtOH/50% DME mixtures below 770 K, the mechanisms predicts a higher reactivity and ignition delay times which are up to 10-20% shorter than experimental results. This suggests that further improvement of the model of ethanol/DME binary fuel is warranted to refine the model's ability to simulate the data over a wider range of conditions. The important reactions controlling both ethanol and DME oxidation chemistry are highlighted in the "brute-force" sensitivity analysis, Fig. 2, and will be discussed here.

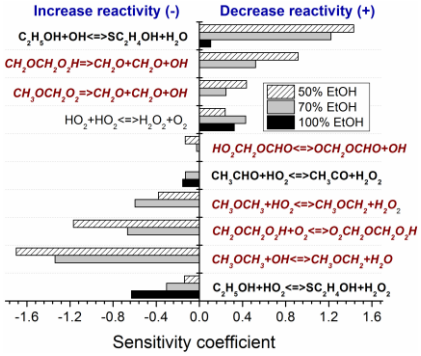

Figure 2: Brute-force" sensitivity analysis to ignition delay times performed at p = 20 atm, φ = 1.0 and T = 770 K for 100% EtOH, and 70/30 and 50/50 EtOH/DME mixtures

3.1 H-atom abstraction

For the 100% EtOH system, H-atom abstraction by $H\dot{O}_2$ radicals at the alpha site on ethanol shows the highest promoting effect on ignition delay times. Unfortunately, neither experimental measurements nor theoretical calculations of this rate constant are so far available in the literature. Therefore, similar to the work of both Mittal et al. [18] and Metcalfe et al.[42], an analogical analysis of the reaction of *n*-butanol with $H\dot{O}_2$ radicals calculated by Zhou et al. [43] was made. Specifically, the total rate of $H\dot{O}_2$ radical consumption *via* H-atom abstractions was increased by a factor of 2 which is higher than the value stated by Mittal et al. (1.75) to better predict the reactivity of ethanol/air mixtures at high pressures (76 bar) reported in [15]. Moreover, the same branching ratio for alpha, beta and $\dot{O}H$ sites proposed by Zhou et al. was applied to estimate rates at the other two abstraction sites.

H-atom abstraction from ethanol by $\dot{O}H$ radicals at the alpha site shows the strongest inhibiting effect and the promotion is more prominent in the presence of DME due to the higher concentrations of $\dot{O}H$ radicals generated from the low temperature chain-branching processes involved in DME oxidation. This observation is similar to our recent study of toluene/DME ignition [33]. The rate constant used in Mittal et al was originally taken from Sivaramakrishnan et al. [44], but the authors increased the A-factor by 25% and maintained the total rate of $\dot{O}H$ consumption *via* H-atom abstraction from ethanol. However this adjustment leads to a relatively large branching ratio (over 90%) for this channel resulting in the prediction of increased concentrations of acetaldehyde and lower concentrations of ethylene compared to the data reported by Li et al. [45]. It is worth noting that the recommendation of Mittal et al. did not agree with the recent measurement (75 – 80% for the branching ratio) by Stranic et al. [46]. In this study, the total rate is adopted from the Stranic et al. measurement which is quite close to Sivaramakrishnan et al. Moreover, the rate constant of the channel forming SC_2H_4OH and H_2O was reduced by 30% to agree with the branching ratio measured by Stranic et al.

3.2 Fuel radical decomposition

The reaction of acetaldehyde with $H\dot{O}_2$ radicals *via* H-atom abstraction promotes reactivity for the 100% EtOH and 70% EtOH/30% DME systems. Mendes et al. [47] calculated the rate constant at the MP2/6-311G(d,p) level of theory combined with conventional transition state theory with an asymmetric Eckart tunneling correction. Their determined value is close to the recommendations of Baulch et al. [48]and da Silva and Bozzelli [49] and it is thus selected to describe this reaction.

It can be clearly seen that with increasing concentrations of DME, the reactions controlling ignition kinetic gradually transition to DME chemistry. The rate constants related to DME low temperature chemistry highlighted in Fig. 2 has been carefully optimized by Burke et al. [40]. However, the decomposition of the carbonyl-hydroperoxide (HO_2CH_2OCHO) forming $\dot{O}CH_2OCHO$ and $\dot{O}H$ radicals still has a large uncertainty. In this study, the rate constant is originally adopted from Sahetchian et al. [50] recommendation which has been used by Burke et al. [40], Curran et al. [51,52] and Zhao et al. [53], but these authors increased the rate constant by a factor of 5, 10 and 24. To achieve a reasonable adjustment, we only increase the rate constant of Sahetchian et al. by a factor of 2.5 which is within the uncertainty of their measurement.

3.3 Well-skipping reactions

3.4 Waddington Mech and second O_2 addition

3.5 Updated model performance

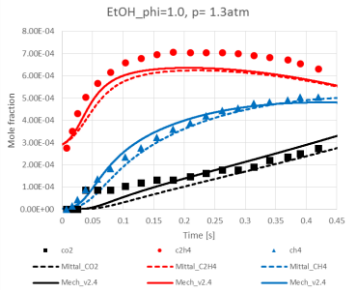

Figure 3: Ethanol FR data 1.3 atm, Φ = 1.3, 950 K

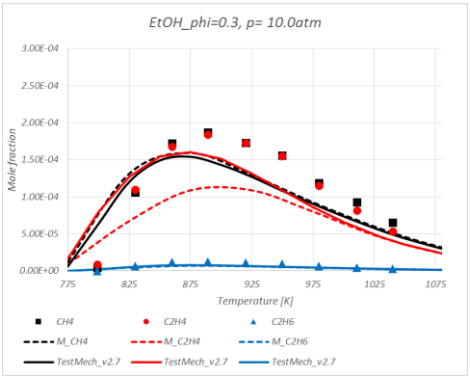

Figure 4: Ethanol JSR data 10 atm, Φ = 0.3 [22]

A detailed comparison of the updated and original models compared to the new experimental data will be discussed in the following section.

4. Results and discussion

All mixtures were tested in the RCM in order to measure the ignition delay times in the low temperature range. For the experiments at higher temperatures, they were performed in the DRIVE-HPST except for the DME mixtures which were previously measured in the NUIG HPST [40]. Moreover, the 100% EtOH mixtures at 20 and 40 atm, at φ = 1.0 were studied in both facilities to allow an inter-comparison of experimental results, with good agreement observed.

4.1 Effect of physical conditions on reactivity of pure fuels

Generally, for the mixtures with a given blending ratio, the experimental trends with respect to the influence on ignition delay time of temperature, pressure and equivalence ratio are very much in-line chemical intuition and will not be discussed in great detail here. The extreme cases of 100% EtOH and 100% DME ignition will be briefly described to highlight the antagonistic behavior of EtOH on DME and/or the promoting effect of DME on EtOH and to provide a basis for discussion of the behaviors of the fuel blends. All of the measured and simulated ignition delay times are provided in Figs. 3–8.

For 100% EtOH the experimental temperature dependence can be essentially correlated using an Arrhenius or modified-Arrhenius type correlation in both the high- and low-temperature regimes without a change in the global activation energy. This is true for all conditions of pressure and equivalence ratio. Both the updated and original

mechanisms are capable of predicting the Arrhenius-type dependence with very little difference between them, as under the conditions studied EtOH shows little or no reactivity at temperatures below 900 K. Hence our need to use a highly-reactive radical initiator, DME, to induce low temperature chemistry in order to shorten ignition times and permit the measurement of ignition delay times.

For 100% DME the ignition delay times show a straight-forward Arrhenius-type dependence on temperature above 1050 K, whereas at temperatures below this a typical NTC behavior can be observed due to its well-established chain-branching reaction mechanism. Again, both models accurately simulate this behavior.

It is clear that the original and updated models are valid in predicting ignition times for ethanol/air mixtures above 800 K and DME/air mixtures over the entire temperature ranges investigated, for all conditions of pressures and equivalence ratios. The fundamental question of this work now arises. Do the models retain their predictability of the experimental measurements beyond the previous validation ranges studied?

4.2 Effect of blending ratio on reactivity

Our results indicate that, the addition of DME exhibits a two-fold effect on ethanol ignition: 1) DME inhibits the reactivity of ethanol at higher temperatures (T > 1050 K) as ethanol undergoes either unimolecular decomposition or beta-H atom abstraction to form the highly reactive species, ethylene and ȮH radicals, which result in accelerated ignition. By contrast, only less reactive species, $\dot{C}H_3$ radicals and formaldehyde are formed in DME oxidation at high temperature *via* either unimolecular decomposition or H-atom abstraction followed by C–O beta scission, resulting in the inhibition of ignition; 2) DME promotes the reactivity of ethanol at lower temperatures (T = 650 – 950 K) where ethanol mainly undergoes alpha-H atom abstraction followed by O–H bond β–scission forming less-reactive acetaldehyde while DME can undergo the low temperature chain-branching process to form abundant ȮH radicals. As a result, DME addition shortens the ignition delay times at lower temperatures, as shown in Figs. 3–8.

Interestingly, the 70% EtOH/30% DME mixtures retain the ignition behavior of ethanol suggesting that ethanol chemistry dominants the ignition kinetics of these mixture even though more reactions involving DME chemistry appear in the sensitivity analysis, Fig. 2. Both models reproduce well the experimental observations. For the 50% EtOH/50% DME mixtures, the ignition behavior is closer to that of pure DME, showing NTC behavior. The original model is capable of predicting the experimental data at temperatures above 910 K but it under-predicts the reactivity at temperature below 910 K. Obviously, the modification in the reaction of HO_2CH_2OCHO decomposition improves agreement in terms of kinetic chemistry of the binary fuel mixtures.

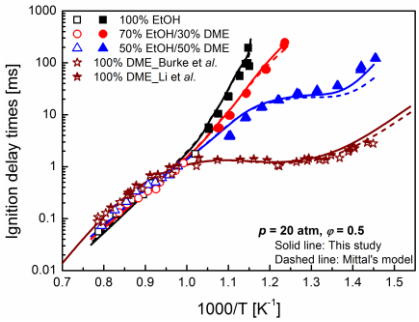

Figure 53: comparison of measured ignition delay times (open symbols: DRIVE-HPST, close symbols: RCM) with model predictions (lines) for measurements of φ = 0.5 and 20 bar.

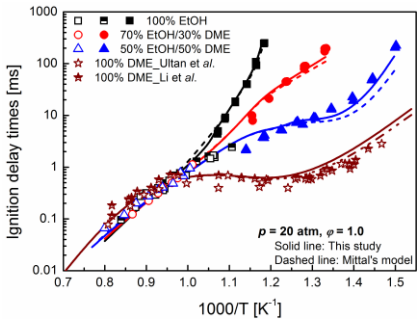

Figure 64: Comparison of measured ignition delay times (open symbols: DRIVE-HPST, close symbols: RCM, half-opened symbols: NUIG-HPST) with model predictions (lines) at φ = 1 and 20 bar.

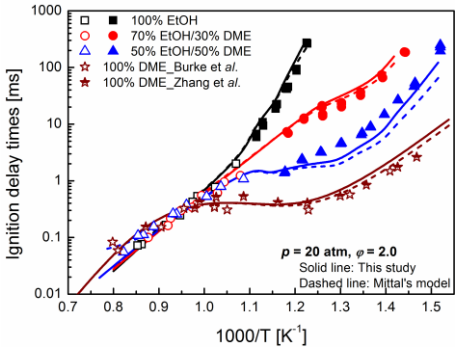

Figure 75: Comparison of measured ignition delay times (open symbols: DRIVE-HPST, close symbols: RCM) with model predictions (lines) at φ = 2 and 20 bar.

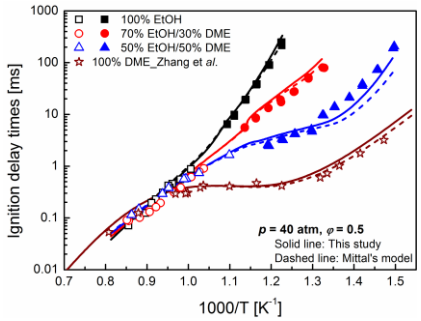

Figure ~~8~~6: Comparison of measured ignition delay times (open symbols: DRIVE-HPST, close symbols: RCM) with model predictions (lines) at φ = 0.5 and 40 bar.

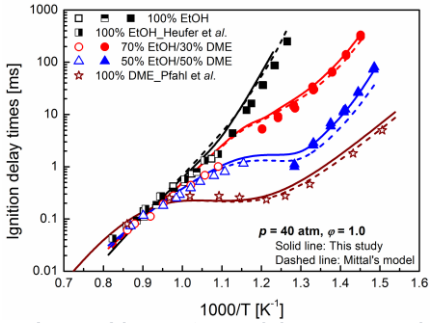

Figure ~~9~~7: Comparison of measured ignition delay times (open symbols: DRIVE-HPST, close symbols: RCM, half-opened symbols: NUIG-HPST) with model predictions (lines) at φ = 1 and 40 bar.

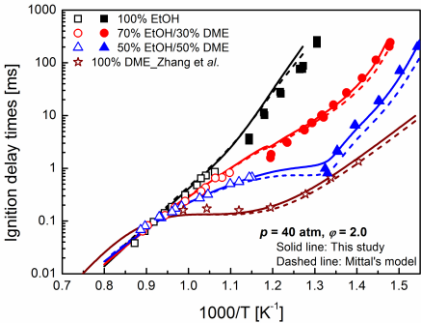

Figure ~~10~~8: Comparison of measured ignition delay times (open symbols: DRIVE-HPST, close symbols: RCM, half-opened symbols: NUIG-HPST) with model predictions (lines) at φ = 1 and 40 bar.

5. Conclusion

Acknowlegments

The DRIVE laboratory thanks French National Research Agency under the ANR project SHOCK (ANR-13-JS09-0013-01) and the Council of Burgundy for their financial support.

References

[1] P.S. Nigam, A. Singh, Production of liquid biofuels from renewable resources, Prog. Energy Combust. Sci. 37 (2011) 52–68. doi:10.1016/j.pecs.2010.01.003.

[2] A. Demirbas, Progress and recent trends in biofuels, Prog. Energy Combust. Sci. 33 (2007) 1–18. doi:10.1016/j.pecs.2006.06.001.

[3] V. Gargiulo, M. Alfè, G. Di Blasio, C. Beatrice, Chemico-physical features of soot emitted from a dual-fuel ethanol–diesel system, Fuel. 150 (2015) 154–161. doi:10.1016/j.fuel.2015.01.096.

[4] M. Matti Maricq, Soot formation in ethanol/gasoline fuel blend diffusion flames, Combust. Flame. 159 (2012) 170–180. doi:10.1016/j.combustflame.2011.07.010.

[5] F.M. Haas, M. Chaos, F.L. Dryer, Low and intermediate temperature oxidation of ethanol and ethanol–PRF blends: An experimental and modeling study, 2009. doi:10.1016/j.combustflame.2009.08.012.

[6] Ö.L. Gülder, Laminar burning velocities of methanol, ethanol and isooctane-air mixtures, Symp. Combust. 19 (1982) 275–281. doi:10.1016/S0082-0784(82)80198-7.

[7] F.N. Egolfopoulos, D.X. Du, C.K. Law, A study on ethanol oxidation kinetics in laminar premixed flames, flow reactors, and shock tubes, Symp. Combust. 24 (1992) 833–841. doi:10.1016/S0082-0784(06)80101-3.

[8] T.S. Kasper, P. Oßwald, M. Kamphus, K. Kohse-Höinghaus, Ethanol flame structure investigated by molecular beam mass spectrometry, Combust. Flame. 150 (2007) 220–231. doi:10.1016/j.combustflame.2006.12.022.

[9] P. Saxena, F.A. Williams, Numerical and experimental studies of ethanol flames, Proc. Combust. Inst. 31 (2007) 1149–1156. doi:10.1016/j.proci.2006.08.097.

[10] K. Eisazadeh-Far, A. Moghaddas, J. Al-Mulki, H. Metghalchi, Laminar burning speeds of ethanol/air/diluent mixtures, Proc. Combust. Inst. 33 (2011) 1021–1027. doi:10.1016/j.proci.2010.05.105.

[11] G. Broustail, P. Seers, F. Halter, G. Moréac, C. Mounaim-Rousselle, Experimental determination of laminar burning velocity for butanol and ethanol iso-octane blends, Fuel. 90 (2011) 1–6. doi:10.1016/j.fuel.2010.09.021.

[12] E. Varea, V. Modica, A. Vandel, B. Renou, Measurement of laminar burning velocity and Markstein length relative to fresh gases using a new postprocessing procedure: Application to laminar spherical flames for methane, ethanol and isooctane/air mixtures, Combust. Flame. 159 (2012) 577–590. doi:10.1016/j.combustflame.2011.09.002.

[13] K. Natarajan, K.A. Bhaskaran, Experimental and analytical investigation of high temperature ignition of ethanol, (1981).

[14] M.P. Dunphy, J.M. Simmie, High-temperature Oxidation of Ethanol Part 1 .-Ignition Delays in Shock Waves, J. CHEM. SOC. FARADAY TRANS. 87 (1991) 1691–1696.

[15] K.A. Heufer, H. Olivier, Determination of ignition delay times of different hydrocarbons in a new high pressure shock tube, Shock Waves. 20 (2010) 307–316. doi:10.1007/s00193-010-0262-2.

[16] L.R. Cancino, M. Fikri, A.A.M. Oliveira, C. Schulz, Measurement and Chemical Kinetics Modeling of Shock-Induced Ignition of Ethanol−Air Mixtures, Energy & Fuels. 24 (2010) 2830–2840. doi:10.1021/ef100076w.

[17] C. Lee, S. Vranckx, K.A. Heufer, S. V. Khomik, Y. Uygun, H. Olivier, R.X. Fernandez, On the Chemical Kinetics of Ethanol Oxidation: Shock Tube, Rapid Compression Machine and Detailed Modeling Study, Zeitschrift Für Phys. Chemie. 226 (2012) 1–28. doi:10.1524/zpch.2012.0185.

[18] G. Mittal, S.M. Burke, V.A. Davies, B. Parajuli, W.K. Metcalfe, H.J. Curran, Autoignition of ethanol in a rapid compression machine, Combust. Flame. 161 (2014) 1164–1171. doi:10.1016/j.combustflame.2013.11.005.

[19] C.L. Barraza-Botet, S.W. Wagnon, M.S. Wooldridge, Combustion Chemistry of Ethanol: Ignition and Speciation Studies in a Rapid Compression Facility, J. Phys. Chem. A. 120 (2016) 7408–7418. doi:10.1021/acs.jpca.6b06725.

[20] F.Z. Li, D.K.S. Chen, SAE TECHNICAL The Solution for Steady State Temperature Distribution in Monolithic Catalytic Converters, (2001).

[21] F. Herrmann, B. Jochim, P. Oßwald, L. Cai, H. Pitsch, K. Kohse-Höinghaus, Experimental and numerical low-temperature oxidation study of ethanol and dimethyl ether, Combust. Flame. 161 (2014) 384–397. doi:10.1016/j.combustflame.2013.09.014.

[22] N. Leplat, P. Dagaut, C. Togbé, J. Vandooren, Numerical and experimental study of ethanol combustion and

oxidation in laminar premixed flames and in jet-stirred reactor, Combust. Flame. 158 (2011) 705–725. doi:10.1016/j.combustflame.2010.12.008.
[23] K.E. Noorani, B. Akih-Kumgeh, J.M. Bergthorson, Comparative High Temperature Shock Tube Ignition of C1−C4 Primary Alcohols, Energy & Fuels. 24 (2010) 5834–5843. doi:10.1021/ef1009692.
[24] F.R. Gillespie, An experimental and modelling study of the combustion of oxygenated hydrocarbons, NUI Galway, 2014.
[25] D.C. Rakopoulos, C.D. Rakopoulos, R.G. Papagiannakis, D.C. Kyritsis, Combustion heat release analysis of ethanol or n-butanol diesel fuel blends in heavy-duty DI diesel engine, Fuel. 90 (2011) 1855–1867. doi:10.1016/j.fuel.2010.12.003.
[26] S. Padala, C. Woo, S. Kook, E.R. Hawkes, Ethanol utilisation in a diesel engine using dual-fuelling technology, Fuel. 109 (2013) 597–607. doi:10.1016/j.fuel.2013.03.049.
[27] C. Olm, T. Varga, É. Valkó, S. Hartl, C. Hasse, T. Turányi, Development of an Ethanol Combustion Mechanism Based on a Hierarchical Optimization Approach, Int. J. Chem. Kinet. 48 (2016) 423–441. doi:10.1002/kin.20998.
[28] M.P. Dunphy, P.M. Patterson, J.M. Simmie, High-temperature oxidation of ethanol. Part 2.—Kinetic modelling, J. Chem. Soc., Faraday Trans. 87 (1991) 2549–2559. doi:10.1039/FT9918702549.
[29] N.M. Marinov, A detailed chemical kinetic model for high temperature ethanol oxidation, Int. J. Chem. Kinet. 31 (1999) 183–220. doi:10.1002/(SICI)1097-4601(1999)31:3<183::AID-KIN3>3.0.CO;2-X.
[30] * Juan Li, and Andrei Kazakov, F.L. Dryer, Experimental and Numerical Studies of Ethanol Decomposition Reactions, (2004). doi:10.1021/JP0480302.
[31] W.K. Metcalfe, S.M. Burke, S.S. Ahmed, H.J. Curran, A Hierarchical and Comparative Kinetic Modeling Study of $C_1 - C_2$ Hydrocarbon and Oxygenated Fuels, Int. J. Chem. Kinet. 45 (2013) 638–675. doi:10.1002/kin.20802.
[32] G.P. Smith, D.M. Golden, M. Frenklach, N.W. Moriarty, B. Eiteneer, M. Goldenberg, T. Bowman, R.K. Hanson, S. Song, J. W.C. Gardiner, V. Lissianski, Z. Qin, http://www.me.berkeley.edu/gri_mech/, (n.d.).
[33] Y. Zhang, K.P. Somers, M. Mehl, W.J. Pitz, R.F. Cracknell, H.J. Curran, Probing the Antagonistic Effect of Toluene as a Component in Surrogate Fuel Models at Low Temperatures and High Pressures. A Case Study of Toluene/Dimethyl Ether Mixtures, in: Proc. Combust. Inst., 2017: p. in press.
[34] L. Brett, J. MacNamara, P. Musch, J.M. Simmie, Simulation of methane autoignition in a rapid compression machine with creviced pistons, Combust. Flame. 124 (2001) 326–329.
[35] S.M. Gallagher, H.J. Curran, W.K. Metcalfe, D. Healy, J.M. Simmie, G. Bourque, A rapid compression machine study of the oxidation of propane in the negative temperature coefficient regime, Combust. Flame. 153 (2008) 316–333.
[36] J. Würmel, J.M. Simmie, CFD studies of a twin-piston rapid compression machine, Combust. Flame. 141 (2005) 417–430.
[37] C. Morley, Gaseq version 0.79, Http://www.gaseq.co.uk/. (2005).
[38] H. El Merhubi, A. Kéromnès, G. Catalano, B. Lefort, L. Le Moyne, A high pressure experimental and numerical study of methane ignition, Fuel. 177 (2016) 164–172. doi:10.1016/j.fuel.2016.03.016.
[39] D. Darcy, C.J. Tobin, K. Yasunaga, J.M. Simmie, J. Würmel, W.K. Metcalfe, T. Niass, S.S. Ahmed, C.K. Westbrook, H.J. Curran, A high pressure shock tube study of n-propylbenzene oxidation and its comparison with n-butylbenzene, Combust. Flame. 159 (2012) 2219–2232. doi:10.1016/j.combustflame.2012.02.009.
[40] U. Burke, K.P. Somers, P. O'Toole, C.M. Zinner, N. Marquet, G. Bourque, E.L. Petersen, W.K. Metcalfe, Z. Serinyel, H.J. Curran, An ignition delay and kinetic modeling study of methane, dimethyl ether, and their mixtures at high pressures, Combust. Flame. 162 (2015) 315–330. doi:10.1016/j.combustflame.2014.08.014.
[41] A. Kéromnès, W.K. Metcalfe, K.A. Heufer, N. Donohoe, A.K. Das, C.-J.J. Sung, J. Herzler, C. Naumann, P. Griebel, O. Mathieu, M.C. Krejci, E.L. Petersen, W.J. Pitz, H.J. Curran, An experimental and detailed chemical kinetic modeling study of hydrogen and syngas mixture oxidation at elevated pressures, Combust. Flame. 160 (2013) 995–1011. doi:10.1016/j.combustflame.2013.01.001.
[42] W.K. Metcalfe, S.M. Burke, S.S. Ahmed, H.J. Curran, A Hierarchical and Comparative Kinetic Modeling Study of C 1 − C 2 Hydrocarbon and Oxygenated Fuels, Int. J. Chem. Kinet. 45 (2013) 638–675. doi:10.1002/kin.20802.
[43] C.-W. Zhou, J.M. Simmie, H.J. Curran, Rate constants for hydrogen abstraction by HȮ2 from n-butanol, Int. J. Chem. Kinet. 44 (2012) 155–164. doi:10.1002/kin.20708.
[44] R. Sivaramakrishnan, M.-C. Su, J. V. Michael, S.J. Klippenstein, L.B. Harding, B. Ruscic, Rate Constants for the Thermal Decomposition of Ethanol and Its Bimolecular Reactions with OH and D: Reflected Shock Tube and Theoretical Studies, J. Phys. Chem. A. 114 (2010) 9425–9439. doi:10.1021/jp104759d.
[45] J. Li, Z.W. Zhao, A. Kazakov, M. Chaos, F.L. Dryer, J.J. Scire, A comprehensive kinetic mechanism for CO, CH2O, and CH3OH combustion, Int. J. Chem. Kinet. 39 (2007) 109–136. doi:10.1002/kin.20218.
[46] I. Stranic, G.A. Pang, R.K. Hanson, D.M. Golden, C.T. Bowman, Shock Tube Measurements of the Rate Constant for the Reaction Ethanol + OH, J. Phys. Chem. A. 118 (2014) 822–828. doi:10.1021/jp410853f.

[47] J. Mendes, C.-W. Zhou, H.J. Curran, Theoretical Chemical Kinetic Study of the H-Atom Abstraction Reactions from Aldehydes and Acids by Ḣ Atoms and ȮH, HȮ$_2$, and ĊH$_3$ Radicals, J. Phys. Chem. A. 118 (2014) 12089–12104. doi:10.1021/jp5072814.
[48] D.L. Baulch, C.J. Cobos, R.A. Cox, C. Esser, P. Frank, T. Just, J.A. Kerr, M.J. Pilling, J. Troe, R.W. Walker, J. Warnatz, Evaluated kinetic data for combustion modeling, J. Phys. Chem. Ref. Data. 21 (1992) 411–734.
[49] G. da Silva, J.W. Bozzelli, Role of the α-hydroxyethylperoxy radical in the reactions of acetaldehyde and vinyl alcohol with HO2, Chem. Phys. Lett. 483 (2009) 25–29. doi:10.1016/j.cplett.2009.10.045.
[50] K.A. Sahetchian, R. Rigny, J. Tardieu de Maleissye, L. Batt, M. Anwar Khan, S. Mathews, The pyrolysis of organic hydroperoxides (ROOH), Symp. Combust. 24 (1992) 637–643. doi:10.1016/S0082-0784(06)80078-0.
[51] S.L. Fischer, F.L. Dryer, H.J. Curran, The reaction kinetics of dimethyl ether. I: High-temperature pyrolysis and oxidation in flow reactors, Int. J. Chem. Kinet. 32 (2000) 713–740. doi:10.1002/1097-4601(2000)32:12<713::AID-KIN1>3.0.CO;2-9.
[52] H.J. Curran, S.L. Fischer, F.L. Dryer, The reaction kinetics of dimethyl ether. II: Low-temperature oxidation in flow reactors, Int. J. Chem. Kinet. 32 (2000) 741–759. doi:10.1002/1097-4601(2000)32:12<741::AID-KIN2>3.0.CO;2-9.
[53] Z. Zhao, M. Chaos, A. Kazakov, F.L. Dryer, Thermal decomposition reaction and a comprehensive kinetic model of dimethyl ether, Int. J. Chem. Kinet. 40 (2008) 1–18. doi:10.1002/kin.20285.